Ab initio exploration of post-PPV transitions in low-pressure analogs of $MgSiO_3$

Koichiro Umemoto[1] and Renata M. Wentzcovitch[2,3]

[1]*Earth-Life Science Institute, Tokyo Institute of Technology, Tokyo, 152-8550, Japan*

[2]*Department of Applied Physics and Applied Mathematics, Columbia University, New York, NY, 10027, USA*

[3]*Department of Earth and Environmental Sciences, Lamont Doherty Earth Observatory, Columbia University, New York, NY, 10964, USA*

(Received 14 September 2019; published 3 December 2019)

Here, we present an *ab initio* investigation of the pressure-induced behavior of $MgGeO_3$ and $NaMgF_3$ perovskite (PV), traditional low-pressure analogs (LPAs) of $MgSiO_3$ PV. The latter is an exceedingly important system in planetary sciences displaying novel phases and phase reactions under pressure that are impractically high and still challenging to experiments. Specifically, we investigate the possibility of $MgGeO_3$ and $NaMgF_3$ to display at lower pressures the novel phases, $I\bar{4}2d$-type A_2BX_4, $P2_1/c$-type AB_2X_5, and dissociation/recombination transitions displayed by $MgSiO_3$ above ∼500 GPa, alone or in the presence of its binary compounds, MgO and SiO_2. We find that, although neither $MgGeO_3$ nor $NaMgF_3$ are perfect LPAs of $MgSiO_3$, they are useful for several reasons: (i) both display the post-PV transition observed in $MgSiO_3$ PV; (ii) starting at ∼20 GPa, the Na-Mg-F system produces a novel $P2_1/c$-type $NaMg_2F_5$ phase by dissociation of $NaMgF_3$ or by its compression with MgF_2. Instead, the Mg-Ge-O system produces a $I\bar{4}2d$-type Mg_2GeO_4 by dissociation of $MgGeO_3$ or by its compression with MgO starting at ∼200 GPa. Such pressures are routinely accessible in laser-heated diamond-anvil cells today; (iii) like $MgSiO_3$, both systems ultimately dissociate into the binary AX and BX_2 compounds, confirming this trend in ternary systems first predicted in $MgSiO_3$. We also predict potential metastable phase transitions into a Gd_2S_3-type structure in $MgGeO_3$ and into a U_2S_3-type structure in $NaMgF_3$. Metastable polymorphic transitions may occur more easily than dissociation/recombination reactions under insufficiently heated compression.

DOI: 10.1103/PhysRevMaterials.3.123601

I. INTRODUCTION

Computational materials discovery and design have been particularly abundant at high pressures. *Ab initio* methods are predictive, and it is considerably less challenging than doing it experimentally. Early successful discoveries in mineral physics gave great impetus to this field [1–3] and propelled the development of materials discovery methods (e.g., Refs. [4–9]). Prediction and experimental confirmation of novel important chemistries (e.g., Refs. [10–13]) and novel electronic states (e.g., Refs. [14–16]) at high pressures and of near-room-temperature superconductivity at 2 Mbar [17–19] are among the latest achievements in this field. These discoveries were impactful because there was great experimental/theoretical synergy that concretely advanced the research front. However, important computational predictions at extreme pressures cannot be easily addressed experimentally.

This is particularly true about planetary materials where the range of pressures and temperatures of practical interest can reach tens of terapascals (TPas) (hundreds of megabars) and 10^4–10^5 K. Experimental techniques have advanced tremendously in recent decades [20–24], but most of the pressure-temperature range of planets larger than Earth are still challenging. For this reason, studies of "low-pressure analogs" (LPAs) of key high-pressure phases have been a common practice in mineral physics. Such analog materials are expected to display similar phase relations and structure-property relations as the experimentally inaccessible high-pressure forms. Today, in this age of exoplanetary discoveries, the search for LPAs is more active than ever. A multitude of exotic planets with unprecedented compositions are being discovered at a fast pace causing a scientific boom in planetary astronomy. Modeling and understanding of these planetary interiors depends fundamentally on the discovery of novel planet forming phases and computations of their properties at extreme conditions.

An especially significant set of unconfirmed mineral physics predictions concerns the nature of "post-post-perovskite" (post-PPV) transitions in $MgSiO_3$. PPV $MgSiO_3$ has the $CaIrO_3$ structure (space group: *Cmcm*) and is the highest pressure form of this major mantle silicate known to exist in the Earth. It should exist in the Earth's mantle beyond ∼2 600-km depth where the pressure is ∼125 GPa and temperatures higher than 2500 K. Between 660- and 2600-km depths, $MgSiO_3$ exists in the *Pbnm* orthorhombic perovskite structure—bridgmanite (Bm). Bm is the most abundant phase on Earth and is responsible for up to ∼50% of its volume.

Terrestrial-type exoplanets, such as Earth, have mantles dominated by silicates and oxides. Among them, large terrestrial exoplanets, frequently referred to as "super Earths," with masses up to ∼13 Earth masses ($M_\oplus$) (or less than Uranus/Neptune masses), are arguably the most interesting exoplanets for their similarities with Earth. Pressures can reach ∼2.5 TPa in their mantles. A series of predictions of post-PPV phase transitions in $MgSiO_3$ and other stoichiometries in the Mg-Si-O system have been made and confirmed by several calculations [8,25–28]. There is no lack of theoretical

consensus on these predictions and the implications for the internal structure of these planets are profound. Planetary modeling using these predictions is also advancing quickly [29,30] but without experimental confirmation these predictions are still speculative. They start at ∼0.5 TPa and proceed to the full dissociation of $MgSiO_3$ into the elementary oxides MgO and SiO_2 at ∼3 TPa at room temperature. At ∼10 000 K, these transition pressures are not much lower, starting at ∼0.3 TPa and full dissociation occurring at ∼2.2 TPa. More importantly, these transitions produce new crystal structures not yet seen in other compounds as far as we know. Given the fundamental importance of these phase transitions to planetary sciences, it is critically important to identify LPAs of $MgSiO_3$ or, more generally, of the Mg-Si-O system.

$NaMgF_3$ perovskite (PV)—neighborite—and $MgGeO_3$ PV have lent themselves as LPAs of $MgSiO_3$ in multiple occasions. They both display the PV-PPV transition like $MgSiO_3$ [31–33]. Furthermore, their binary constituents, NaF/MgO and MgF_2/GeO_2, also display similar pressure-induced behavior as MgO and SiO_2 [34,35]. This is essential because predicted post-PPV transitions in $MgSiO_3$ involve dissociation or recombination reactions of $MgSiO_3$ with its binary oxides.

Using *ab initio* methods, here, we investigate the ability of $MgGeO_3$ and $NaMgF_3$ to produce, at much lower pressures, the novel phases and phase transitions predicted by compression of $MgSiO_3$ to extreme pressures expected in the interiors of super Earths. Next section briefly describes the methods used. Section III describes the predicted post-PPV transitions in the Mg-Si-O system identified so far and the crystal structures involved. Section IV presents results on the Mg-Ge-O and Na-Mg-F systems and discusses the similarities and differences with the Mg-Si-O system. In the final section, we summarize our results and conclusions.

II. COMPUTATIONAL METHODS

Calculations were performed using the local-density approximation (LDA) [36] to density-functional theory. For all atomic species, Vanderbilt-type pseudopotentials [37] were generated. The valence electron configurations and cutoff radii for the pseudopotentials were $2s^2 2p^6 3s^1$ and 1.6 a.u. for Na, $2s^2 2p^6 3s^2$ and 1.6 a.u. for Mg, $2s^2 2p^5$ and 1.6 a.u. for F, $4s^2 4p^1 3d^{10}$ and 1.6 a.u. for Ge, and $2s^2 2p^4$ and 1.4 a.u. for O, respectively. Cutoff energies for the plane-wave expansion are 60 and 70 Ry for Na-Mg-F and Mg-Ge-O systems, respectively. **k**-point meshes for calculations in all phases were sufficiently dense to achieve energy convergence within 1 mRy per formula unit (f.u.). For structural optimization under arbitrary pressures, we used the variable-cell-shape damped molecular dynamics [38,39]. Dynamical matrices were calculated at various wave vectors using density-functional perturbation theory [40,41]. Force constant matrices were obtained to build dynamical matrices at arbitrary q vectors. The vibrational contribution to the free energy was calculated using the quasiharmonic approximation [42] using the QHA software [43]. Also, **q**-point meshes were sufficiently dense to achieve energy convergence within 1 mRy/f.u. All calculations were performed using the QUANTUM-ESPRESSO software [44].

III. THE Mg-Si-O SYSTEM

Several *ab initio* computational studies have addressed transitions involving PPV in the Mg-Si-O system [2,3,8,25–28]. The predicted transitions are as follows:

(1) $MgSiO_3$ (PV) → $MgSiO_3$ (PPV) at ∼0.08 TPa,
(2) $MgSiO_3$ (PPV) → Mg_2SiO_4 ($I\bar{4}2d$-type) + $MgSi_2O_5$ ($P2_1/c$-type) at ∼0.75 TPa,
(3) Mg_2SiO_4 ($I\bar{4}2d$-type) + $MgSi_2O_5$ ($P2_1/c$-type) → Mg_2SiO_4 ($I\bar{4}2d$-type) + SiO_2 (Fe_2P type) at ∼1.3 TPa, and
(4) Mg_2SiO_4 ($I\bar{4}2d$-type) + SiO_2 (Fe_2P-type) → MgO($B2$-type) + SiO_2 (Fe_2P-type) at ∼3.1 TPa.

These pressures were obtained with static *ab initio* LDA calculations which underestimate transition pressures by several gigapascals. All crystal structures involved are indicated in Fig. 1 along with their cation coordinations. The Gd_2S_3-type and U_2S_3-type structures are also relevant because they might be observed experimentally more easily as metastable polymorphs than the dissociated phases. They have been identified as potential high-pressure forms of ABX_3 compounds as well [27,45].

Transition (1) was found in 2004 and revolutionized understanding of Earth's deep mantle [1–3]. Transition (2) is the predicted breakdown of PPV into Mg-rich and Si-rich polymorphs [8,28]. These phases have not yet been identified in other materials. However, the structure of $I\bar{4}2d$-type Mg_2SiO_4 is related to that of Zn_2SiO_4 (II) [46]. Although the cation arrangements in Zn_2SiO_4 (II) are identical to those of $I\bar{4}2d$-type Mg_2SiO_4, the anion arrangement differs. Mg and Si in $I\bar{4}2d$-type Mg_2SiO_4 are eightfold coordinated, whereas Zn and Si atoms in Zn_2SiO_4 (II) have tetrahedral coordination. In transition (3) the Si-rich polymorph breaks down into SiO_2 plus the Mg-rich polymorph [8,28]. The latter has a very broad stability field and is the last ternary phase before the breakdown into the binary oxides at 3.1 TPa as in transition (4) [8]. Reference [28] shows that the last breakdown should occur at ∼2.3 TPa, a rather lower pressure than Ref. [8], leading to the crossing of the two phase boundaries of the transitions (3) and (4) at a temperature above ∼6000 K. Consequently, Ref. [28] proposes a dissociation of Mg_2SiO_4 into $MgSi_2O_5$ and MgO above ∼6000 K, instead of the transition (3).

It happens that the Mg/Si abundance ratio varies within and across planetary mantles and $MgSiO_3$ can coexist with different amounts of MgO or SiO_2 and their coexisting behavior under pressure should also be addressed. The relevant phases of MgO and SiO_2 are also indicated in Fig. 1. When $MgSiO_3$ PPV coexists with $B1$-type MgO or pyrite-type SiO_2, the following recombination reactions occur [27]:

(5) $MgSiO_3$ (PPV) + MgO($B1$-type) → Mg_2SiO_4 ($I\bar{4}2d$-type) at 0.49 TPa and
(6) $MgSiO_3$ (PPV) + SiO_2 (pyrite-type) → $MgSi_2O_5$ ($P2_1/c$-type) at 0.62 TPa.

These recombination reactions are unexpected. Mg_2SiO_4 polymorphs dominate the Earth's mantle up to 23 GPa when its spinel form, ringwoodite, breaks down into $MgSiO_3$ PV and $B1$-type MgO. This postspinel transition produces a major seismic discontinuity at 660-km depth and defines the upper boundary of the Earth's lower mantle. The recombination of $MgSiO_3$ with MgO in (5) and with SiO_2 in (6) at higher

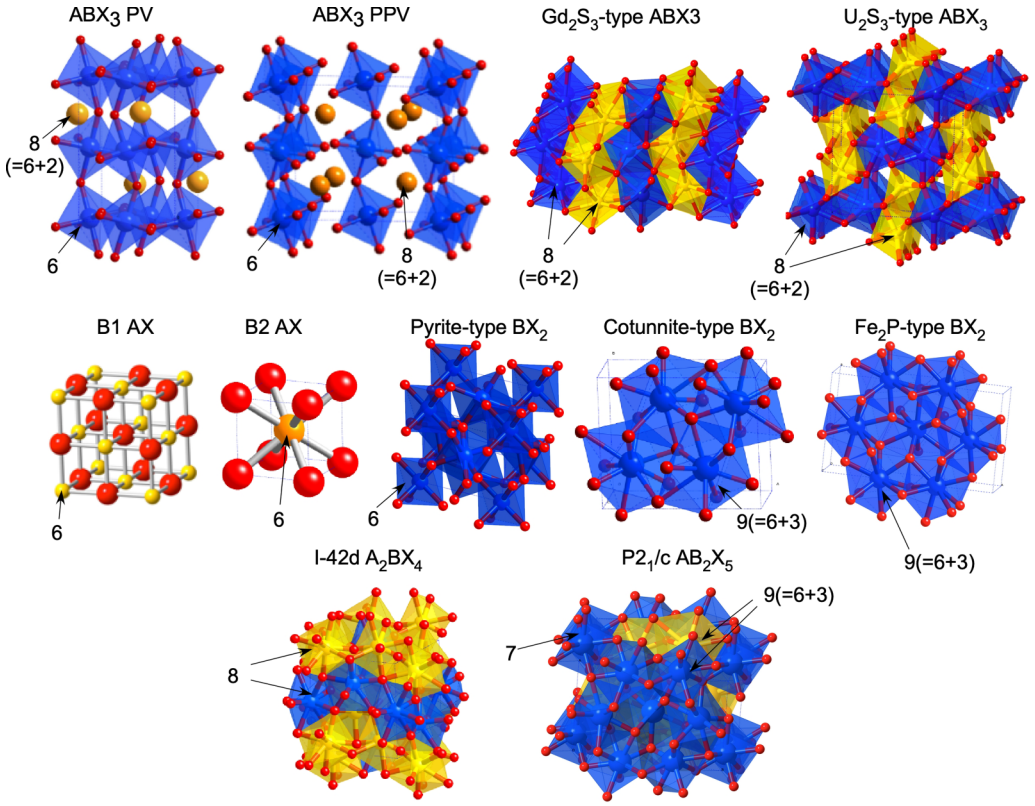

FIG. 1. Crystal structures investigated in the present paper. Yellow and blue spheres or polyhedra denote *A* and *B* cations and coordinations. Red small spheres denote anions *X*. The numerals indicates coordination numbers of cations *A* and *B*. In the ABX_3 PV and PPV structures, *A* and *B* ions are located in approximately bicapped triangular prisms and octahedra. In Gd_2S_3-type and U_2S_3-type ABX_3, both *A* and *B* ions are located in bicapped triangular prisms. For BX_2, the structural unit is octahedra in the pyrite-type phase and a tricapped triangular prism. In $P2_1/c$ AB_2X_5, the *A* cations are at the center of tricapped triangular prisms. There are two kinds of *B* cations; they are at the center of capped triangular prisms and tricapped triangular prisms.

pressures are both surprising since the trend with pressure is clearly toward dissociation into binary oxides. Despite the lack of experimental confirmation, these phase transitions are already being used to model the internal structure and dynamics of super-Earth-type planets [29,30]. Therefore, experimental confirmation of these transitions and phases in LPAs has become quite a pressing issue. These transitions are concisely depicted in Fig. 2.

IV. RESULTS AND DISCUSSION

In this paper, we investigated the relevant structures identified in the Mg-Si-O system and indicated in Fig. 1. They are PV (*Pbnm*), PPV (*Cmcm*), U_2S_3-type (*Pnma*, isostructural with Sb_2S_3-type), and Gd_2S_3-type (*Pnma*, isostructural with La_2S_3-type) for ABX_3-type compounds. The last two structures are important polymorphs of $MgSiO_3$ and of other ABX_3 compounds, more generally [47]. For A*X*-type compounds (MgO and NaF), we included *B*1-type and *B*2-type structures. For BX_2 (GeO_2 and MgF_2), we included pyrite-type ($Pa\bar{3}$), cotunnite-type (*Pnma*), and Fe_2P-type ($P\bar{6}2m$) structures. These are the most important phases in such binaries that combine with the PV or PPV phases at high pressures [27]. For A_2BX_4 (Mg_2GeO_4 and Na_2MgF_4) and AB_2X_5 ($MgGe_2O_5$ and $NaMg_2F_5$) stoichiometries, we included the same $I\bar{4}2d$-type Mg_2SiO_4 and $P2_1/c$-type $MgSi_2O_5$ structures [8,26,28]. None of these phases display soft phonon modes in the reported pressure ranges as shown in Figs. S1 and S2 in the Supplemental Material [48], enabling us to compute free energies and predict high-temperature phase boundaries using the quasiharmonic approximation. All of these phases have nonmetallic band structures with considerably large band gaps (Figs. S3 and S4 in the Supplemental Material [48]). As expected, band dispersions increase under compression.

A. The Mg-Ge-O system

First, we address the elementary oxides. MgO undergoes the *B*1-*B*2 phase transition [49] at 502 GPa, consistent with several theoretical predictions (e.g., Refs. [25,50–53]). Our present calculations indicate that pyrite-type GeO_2 undergoes successive phase transitions to a cotunnite-type structure (257 GPa) followed by an Fe_2P-type structure (534 GPa), in agreement with a previous study [54]. Therefore, GeO_2 is not an exact analog of SiO_2, but it is not too different either. SiO_2 undergoes a direct pyrite to Fe_2P-type transition at low temperatures [55,56]. The sequence of transitions in GeO_2 is only seen in SiO_2 above ~2500 K [56].

Under pressure, $MgGeO_3$ (PPV) is predicted to dissociate into GeO_2 (pyrite) and Mg_2GeO_4 ($I\bar{4}2d$) at 175 GPa [see Fig. 3(a)]. The Mg coordination number is 8 before and after the transition, but the coordination polyhedra are quite

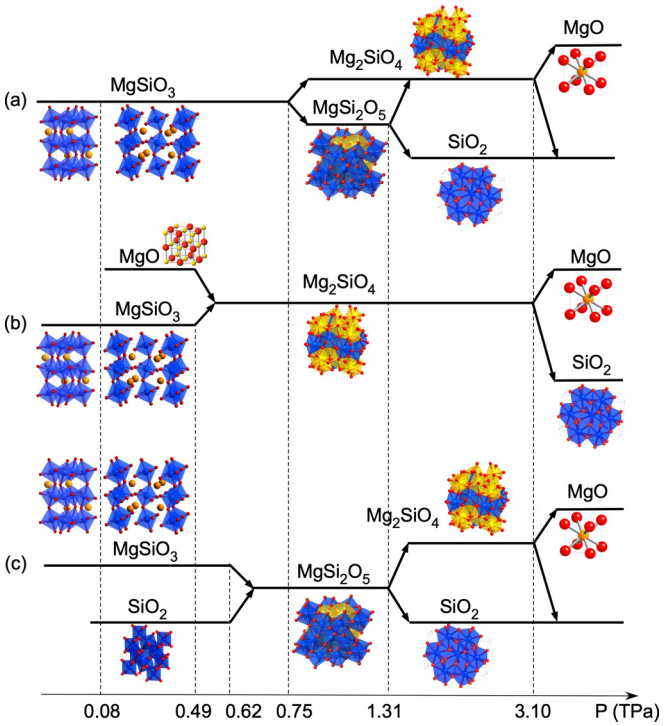

FIG. 2. Pressure-induced post-PPV phase transitions predicted in the Mg-Si-O system as indicated in (a) reactions 1–4, (b) reaction 5, and (c) reaction 6 [1–3,8,27,28]. The indicated transition pressures were obtained using the static LDA and ultrasoft pseudopotentials especially generated for these high-pressure calculations [25]. LDA is known to underestimate transition pressures by ∼5–10 GPa in the Mg-Si-O system [3,25].

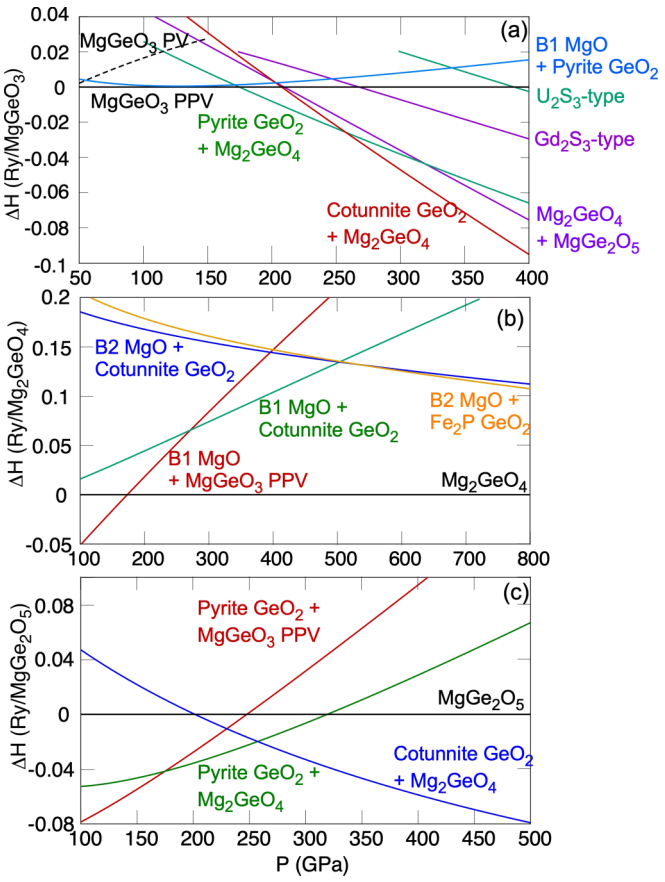

FIG. 3. Relative static enthalpies of (a) aggregation of possible dissociation products of $MgGeO_3$ and other polymorphs (U_2S_3-type and Gd_2S_3-type) of $MgGeO_3$ with respect to $MgGeO_3$ PPV, (b) aggregation of possible dissociation products of Mg_2GeO_4 with respect to $I\bar{4}2d$-type Mg_2GeO_4, and (c) aggregation of possible dissociation products of $MgGe_2O_5$ with respect to $P2_1/c$-type $MgGe_2O_5$.

different (Fig. 1). This behavior means that $MgGeO_3$ skips transition (2) seen in the Mg-Si-O system. Transition (2) is only a metastable transition in $MgGeO_3$ [see Fig. 3(a)]. After the dissociation, pyrite-type GeO_2 transforms to a cotunnite-type phase (257 GPa) and to an Fe_2P-type phase (534 GPa). Dissociation of Mg_2SiO_4 into the elementary oxides is not observed in our calculations up to 800 GPa. The small free-energy difference of 3 to 4 meV/f.u. between $MgGeO_3$ (PPV) and $MgO(B1) + GeO_2$ (pyrite) at 125 GPa [Fig. 3(a)] increases to 23 and 58 meV/f.u. at 0 and 1000 K, respectively, after inclusion of vibrational effects. Therefore, this direct dissociation of the PPV phase into simple oxide is unlikely to materialize experimentally.

When $MgGeO_3$ (PPV) coexists with MgO ($B1$), they recombine into Mg_2GeO_4 ($I\bar{4}2d$) at 173 GPa [Fig. 3(b)]. Simple extrapolation of enthalpy differences suggests that dissociation of Mg_2GeO_4 into MgO ($B2$) and GeO_2 (Fe_2P-type) might occur at ∼3 TPa. When $MgGeO_3$ (PPV) coexists with GeO_2 (pyrite), still no recombination into $MgGe_2O_5$ occurs [Fig. 3(c)]. Only the dissociation of $MgGeO_3$ shown in Fig. 3(a) occurs followed by transitions in GeO_2.

Dissociation and recombination reactions as predicted here are often kinetically inhibited. For example, an x-ray-diffraction (XRD) experiment in $MgGeO_3$ PPV under pressure [57] reported no phase transitions up to 201 GPa at temperatures as high as ∼1600 K. This pressure is quite higher than the dissociation pressure predicted here at ∼175 GPa, suggesting kinetic inhibition even at such high temperatures. Higher temperatures and longer observation times might be required to produce the dissociation of $MgGeO_3$. If this does not happen, $MgGeO_3$ PPV may transform to the Gd_2S_3-type phase at 268 GPa, similar to the case of $MgSiO_3$ [27]. The U_2S_3-type phase, another candidate metastable post-PPV polymorph, has higher enthalpy than Gd_2S_3-type [Fig. 3(a)] and should not be the preferred metastable phase.

Since all phases indicated in Fig. 3 are dynamically stable displaying no soft phonon modes in the relevant pressure ranges, we were able to compute high-temperature phase diagrams using the quasiharmonic approximation (Fig. 4). The dissociation and recombination phase boundaries have negative Clapeyron slopes, which is typical for phase transitions accompanied by increases in coordination numbers and bond lengths along with an overall decrease in phonon frequencies (Fig. S1 in the Supplemental Material [48]). The possible metastable PPV to the Gd_2S_3-type phase boundary has a positive Clapeyron slope at lower temperatures turning into negative above ∼2000 K. This positive Clapeyron slope with increased coordination numbers below ∼2000 K is an exception. This is caused by the upward shift of acoustic phonon frequencies across the PPV-Gd_2S_3 transition which dominates the vibrational energy at lower temperatures. Above

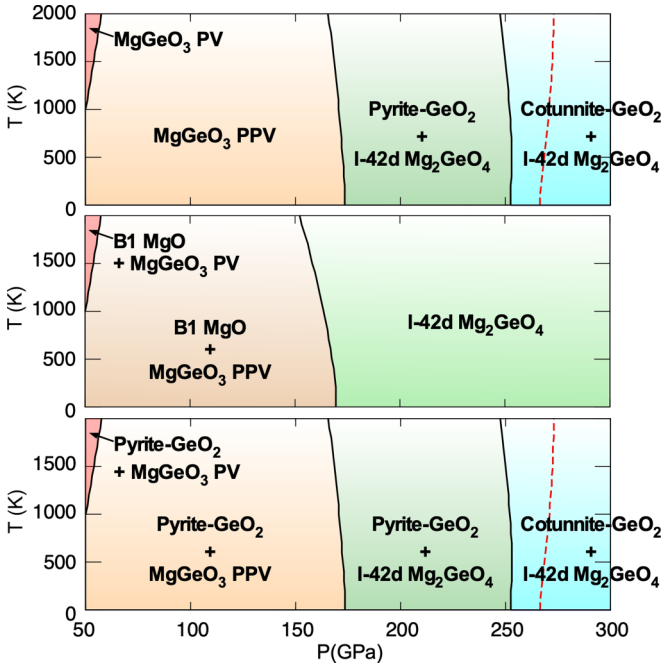

FIG. 4. Phase boundaries of pressure-induced phase transitions in (a) $MgGeO_3$, (b) $MgGeO_3$ and MgO, and (c) $MgGeO_3$ and GeO_2, both cases with the molar ratio of 1:1. In (a), the red dashed line denotes the metastable phase boundary between PPV and Gd_2S_3 type.

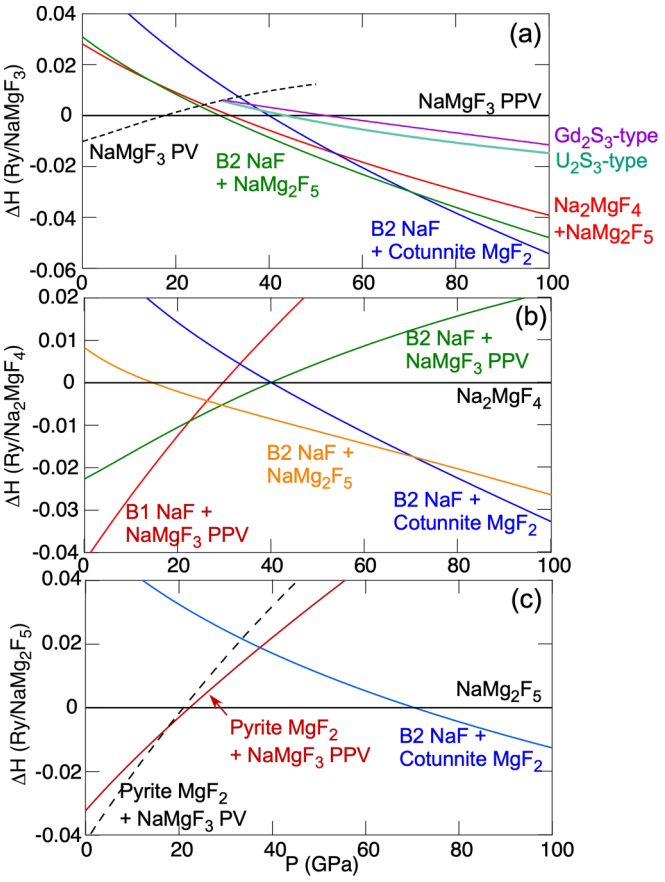

FIG. 5. Relative static enthalpies of (a) aggregation of possible dissociation products of $NaMgF_3$ and other polymorphs (U_2S_3 type and Gd_2S_3 type) of $NaMgF_3$ with respect to $NaMgF_3$ PPV, (b) aggregation of possible dissociation products of Na_2MgF_4 with respect to $I\bar{4}2d$-type Na_2MgF_4, and (c) aggregation of possible dissociation products of $NaMg_2F_5$ with respect to $P2_1/c$-type $NaMg_2F_5$.

~2000 K, the effect of the downward shift of high-frequency optical modes dominates, leading to the negative Clapeyron slope. Zero-point motion (ZPM) decreases the static transition pressures slightly.

B. The Na-Mg-F system

NaF is a LPA of MgO, undergoing the $B1$-$B2$ transition at 27 GPa [34]. MgF_2 is frequently seen as a LPA of SiO_2 and GeO_2. It has the rutile-type structure at ambient pressure and undergoes a series of pressure-induced transitions similar to those in SiO_2 and GeO_2: rutile-type to $CaCl_2$-type at 9.1 GPa, to pyrite-type at 14 GPa, and to cotunnite-type at 36 GPa [35]. The latter occurs in GeO_2 but only at higher temperature in SiO_2 [55,56]. $NaMgF_3$ underdoes the PV-PPV transition at 19.4 GPa [32]. As previously reported [58], our calculated transition pressures are in good agreement with measurements.

Here, we predict that after the PV-PPV transition at 18 GPa, $NaMgF_3$ PPV dissociates into $B1$-type NaF + $P2_1/c$-type $NaMg_2F_5$ at 29 GPa, followed by the full dissociation of $NaMg_2F_5$ into binary fluorides, $B2$-type NaF + cotunnite-type MgF_2, at 71 GPa [Fig. 5(a)]. If $NaMgF_3$ PPV coexists with pyrite-type MgF_2, they combine into $P2_1/c$-type $NaMg_2F_5$ at 22 GPa [Fig. 5(c)]. This recombination pressure is lower than the PPV dissociation pressure (29 GPa). Therefore, the stability field of the PPV phase shrinks when it coexists with MgF_2. The $I\bar{4}2d$-type Na_2MgF_4 phase is dynamically stable above 20 GPa, but it is metastable throughout the entire pressure range examined here [Fig. 5(b)] and is not involved in any of the post-PPV phase transitions. This feature contrasts with the behavior of the Mg-Ge-O system, which stabilizes the A_2BX_4-type phase instead of the AB_2X_5 type. If the dissociations are kinetically inhibited, We predict that $NaMgF_3$ PPV should transform to the metastable U_2S_3-type phase at 43 GPa [Fig. 5(a)]. This transition also occurs in Al_2O_3 [59], where A and B cations are the same and contrasts with the behavior in $MgGeO_3$ where the Gd_2S_3-type phase is the energetically favored metastable phase. Reference [60] also predicted a U_2S_3-type phase to be metastable with respect to the dissociation products, whereas Ref. [61] reported a metastable Gd_2S_3-type phase as post-PPV. The latter study did not investigate the U_2S_3-type phase.

The experimental high-pressure behavior of $NaMgF_3$ PPV has been controversial. No dissociation was reported up to ~70 GPa by Ref. [62], which could not resolve a post-PPV "N phase" or by Ref. [63]. However, a very recent XRD experiment [64] reported the following sequence of phase transitions: $NaMgF_3$ PV → $NaMgF_3$ PPV → U_2S_3-type $NaMgF_3$ → $B2$-type NaF + $P2_1/c$-type $NaMg_2F_5$ → $B2$-type NaF + cotunnite-type MgF_2. Experimentally the dissociation was found only upon heating to very high temperatures. This behavior and the presence of the U_2S_3-type phase suggests kinetic inhibition of the predicted dissociation transition. The experimental transition pressure to the U_2S_3-type phase at

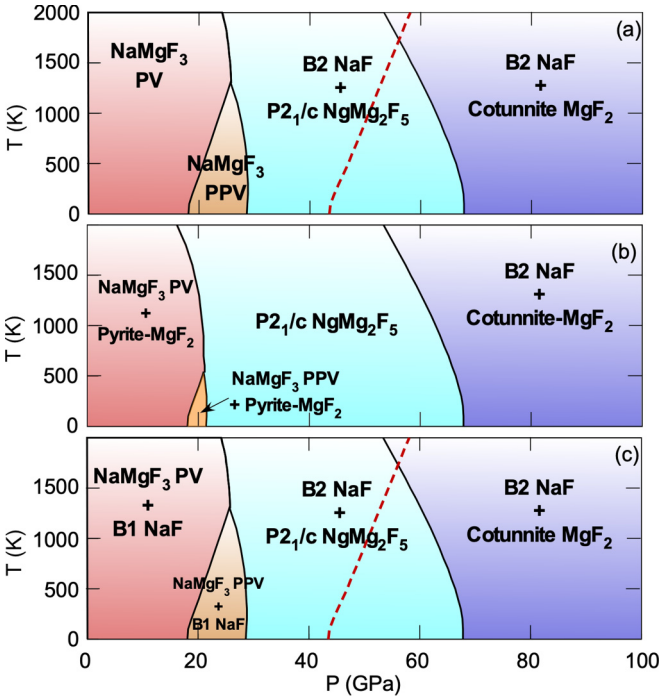

FIG. 6. Phase boundaries of pressure-induced phase transitions in (a) $NaMgF_3$, (b) $NaMgF_3$ and NaF and (c) $NaMgF_3$ and MgF_2, both with the molar ratio of 1:1. Below 1000 K, panel (a) is identical to that reported by Ref. [67]. In (a), the red dashed line denotes the metastable phase boundary between the PPV and the U_2S_3-type phase. For the sake of simplicity, we omit low-pressure phases of MgF_2 below pyrite type and an experimental phase boundary of $NaMgF_3$ perovskite between orthorhombic and cubic phases [66].

room temperature was reported to be 58 GPa, agreeing with our LDA predicted value, 46 GPa at 300 K; this degree of underestimation of transition pressure is typical of the LDA calculations [65]. Although our predictions are qualitatively consistent with the experiment in Ref. [64], we should note a non-negligible difference in dissociation pressures between the experiments and the calculations. Reference [64] reported high-temperature (>2000 K) dissociations into $NaMg_2F_5$ and NaF and into NaF and MgF_2 at pressures beyond ~90 and ~160 GPa, respectively. These dissociation pressures are much higher than our predicted values which still suggest the presence of hysteresis in the experiments. Further investigations will be necessary both computationally and experimentally to elucidate the origin of this discrepancy. From the computational viewpoint, anharmonic contributions to the free energy might also shift the transition pressure. This effect was not considered here and is beyond the scope of the present paper but should be investigated in the future.

Thermodynamic phase boundaries involving these phases in the Na-Mg-F system are shown in Fig. 6. As in the Mg-Ge-O system, ZPM decreases slightly the dissociation/recombination pressures. As in $MgSiO_3$ and $MgGeO_3$, dissociation and recombination have negative Clapeyron slopes, whereas the PV-PPV and the metastable PPV-U_2S_3-type transitions have positive slopes. The stability field of the PPV phase is rather small and closes at 1300 K. When $NaMgF_3$ and MgF_2 coexist, the PPV stability field shrinks closing at ~500 K. At higher temperatures, the PV phase directly dissociates or combines with MgF_2. It should be noted that we have not considered the cubic phase of $NaMgF_3$ PV, a high-temperature and low-pressure form of $NaMgF_3$ PV [66] stabilized by anharmonic effects. As such, phase boundaries of the PV phase at high temperatures might be affected by anharmonicity.

V. SUMMARY AND CONCLUSIONS

This *ab initio* study shows that neither $MgGeO_3$ nor $NaMgF_3$ are perfect LPAs of $MgSiO_3$ as far as post-PPV transitions are concerned. However, at lower pressures achievable routinely in diamond-anvil cells, both compounds produce the new types of phases $I\bar{4}2d$-type A_2BX_4 and $P2_1/c$-type AB_2X_5, predicted in $MgSiO_3$ at very high pressures. Lower transition pressures in these systems other than $MgSiO_3$ can be attributed to cation sizes: For the A site, the ionic radius of Na (r_A) is larger than that of Mg; as for the B site, Ge and Mg ionic radii (r_B) are larger than that of Si. The preference for different high-pressure phase assemblages is related with different r_A/r_B ratios in these systems. The Mg-Ge-O system produces Mg_2GeO_4 by dissociation of $MgGeO_3$ or by its simultaneous compression with MgO. The Na-Mg-F system produces $NaMg_2F_5$ by dissociation of $NaMgF_3$ or by its simultaneous compression with MgF_2. As in $MgSiO_3$, both systems ultimately dissociate into the binary AX and BX_2 compounds. This full dissociation in the Na-Mg-F system is expected at ~80–90 GPa, whereas in the Mg-Ge-O, it is not expected up to ~3 TPa.

When compared with experimental data, our results suggest the possibility of kinetically inhibited transitions in both systems. $MgGeO_3$ could display a metastable transition from the PPV to the Gd_2S_3-type phase, whereas $NaMgF_3$ might display a metastable transition to the U_2S_3-type phase. The latter is also predicted as a stable phase by compression of PPV Al_2O_3 at ~0.37 GPa [59].

Despite the differences, $MgGeO_3$ and $NaMgF_3$ are useful LPAs of $MgSiO_3$ for several reasons. Confirmation of the present predictions would lend further credibility to the pressure induced behavior of $MgSiO_3$, an extremely challenging system to investigate experimentally because of the extreme pressures involved (>500 GPa). In addition, these systems may be useful for future study of effects of secondary but important alloying elements (Fe, Al, and so forth) which must play an important role in super Earths whose mantles should consist of Fe- and Al-bearing Mg-Si-O systems. Furthermore, they are good systems for the exploration and further understanding of metastable phase transitions caused by kinetic inhibition of dissociation and recombination transitions upon cold compression/decompression. This exercise can facilitate future experimental explorations at more challenging pressures and temperatures in the fundamentally important system in planetary sciences—Mg-Si-O.

ACKNOWLEDGMENTS

The authors acknowledge helpful discussions with T. S. Duffy and R. Dutta. K.U. acknowledges support from

JSPS Kakenhi Grant No. 17K05627 and MEXT as "Exploratory Challenge on Post-K computer" (Challenge of Basic Science Exploring Extremes through Multi-Physics and Multi-Scale Simulations). All calculations were performed at the Global Scientific Information and Computing Center and in the ELSI supercomputing system at the Tokyo Institute of Technology. R.M.W. acknowledges National Science Foundation Grants No. EAR-1503084 and No. EAR-1918126.

[1] M. Murakami, K. Hirose, K. Kawamura, N. Sata, and Y. Ohishi, Post-perovskite phase transition in $MgSiO_3$, Science **304**, 855 (2004).

[2] A. R. Oganov and S. Ono, Theoretical and experimental evidence for a post-perovskite phase of $MgSiO_3$ in Earth's D"layer, Nature (London) **430**, 445 (2004).

[3] T. Tsuchiya, J. Tsuchiya, K. Umemoto, and R. M. Wentzcovitch, Phaset ransition in $MgSiO_3$ perovskite in the earth's lower mantle, Earth Planet. Sci. Lett. **224**, 241 (2004).

[4] C. W. Glass, A. R. Oganov, and N. Hansen, USPEX-Evolutionary crystal structure prediction, Comput. Phys. Commun. **175**, 713 (2006).

[5] D. C. Lonie and E. Zurek, XTALOPT: An open-source evolutionary algorithm for crystal structure prediction, Comput. Phys. Commun. **182**, 372 (2011).

[6] C. J. Pickard and R. J. Needs, *Ab initio* random structure searching, J. Phys.: Condens. Matter **23**, 053201 (2011).

[7] Y. Wang, J. Lv, L. Zhu, and Y. Ma, CALYPSO: A method for crystal structure prediction, Comput. Phys. Commun. **183**, 2063 (2012).

[8] S. Q. Wu, M. Ji, C. Z. Wang, M. C. Nguyen, X. Zhao, K. Umemoto, R. M. Wentzcovitch, and K. M. Ho, An adaptive genetic algorithm for crystal structure prediction, J. Phys.: Condens. Matter **26**, 035402 (2014).

[9] F. Curtis, X. Li, T. Rose, Á Vázquez-Mayagoitia, S. Bhattachary, L. M. Ghiringhelli, and N. Marom, GAtor: A first-principles genetic algorithm for molecular crystal structure prediction, J. Chem. Theory Comput. **14**, 2246 (2018).

[10] E. Zurek, R. Hoffmann, N. W. Ashcroft, A. R. Oganov, and A. O. Lyakhov, A little bit of lithium does a lot for hydrogen, Proc. Natl. Acad. Sci. USA **106**, 17640 (2009).

[11] W. Zhang, A. R. Oganov, A. F. Goncharov, Q. Zhu, S. E. Boulfelfel, A. O. Lyakhov, E. Stavrou, M. Somayazulu, V. D. Prakapenka, and Konôpková, Unexpected stable stoichiometries of sodium chlorides, Science **342**, 1502 (2013).

[12] G. L. Weerasinghe, C. J. Pickard, and R. J. Needs, Computational searches for iron oxides at high pressures, J. Phys.: Condens. Matter **27**, 455501 (2015).

[13] Q. Hu, D. Y. Kim, W. Yang, L. Yang, Y. Meng, L. Zhang, and H. K. Mao, FeO_2 and FeOOH under deep lower-mantle conditions and Earth's oxygen-hydrogen cycles, Nature (London) **534**, 241 (2016).

[14] Y. Ma, M. Eremets, A. R. Oganov, Y. Xie, I. Trojan, S. Medvedev, A. O. Lyakhov, M. Valle, and V. Prakapenka, Transparent dense sodium, Nature (London) **458**, 182 (2019).

[15] X. Dong, A. R. Oganov, A. F. Goncharov, E. Stavrou, S. Lobanov, G. Saleh, G. R. Qian, Q. Zhu, C. Gatti, V. L. Deringer, R. Dronskowski, X. F. Zhou, V. B. Prakapenka, Z. Konôpková, I. A. Popov, A. I. Boldyrev, and H. T. Wang, A stable compound of helium and sodium at high pressure, Nat. Chem. **9**, 440 (2017).

[16] Y. Zhang, H. Wang, Y. Wang, L. Zhang, and Y. Ma, Computer-Assisted Inverse Design of Inorganic Electrides, Phys. Rev. X **7**, 011017 (2017).

[17] Y. Li, J. Hao, H. Liu, Y. Li, and Y. Ma, The metallization and superconductivity of dense hydrogen sulfide, J. Chem. Phys. **140**, 174712 (2014).

[18] A. P. Drozdov, M. I. Eremets, I. A. Troyan, V. Ksenofontov, and S. I. Shylin, Conventional superconductivity at 203 kelvin at high pressures in the sulfur hydride system, Nature (London) **525**, 73 (2015).

[19] H. Liu, I. I. Naumov, R. Hoffmann, N. W. Ashcroft, and R. J. Hemley, Potential high-T_c superconducting lanthanum and yttrium hydrides at high pressure, Proc. Natl. Acad. Sci. USA **114**, 6990 (2017).

[20] R. F. Smith, J. H. Eggert, R. Jeanloz, T. S. Duffy, D. G. Braun, J. R. Patterson, R. E. Rudd, J. Biener, A. E. Lazicki, A. V. Hamza, J. Wang, T. Braun, L. X. Benedict, P. M. Celliers, and G. W. Collins, Ramp compression of diamond to five terapascals, Nature (London) **511**, 330 (2014).

[21] L. Dubrovinsky, N. Dubrovinskaia, V. B. Prakapenka, and A. M. Abakumov, Implementation of micro-ball nanodiamond anvils for high-pressure studies above 6 Mbar, Nat. Commun. **3**, 1163 (2012).

[22] N. Dubrovinskaia, L. Dubrovinsky, N. A. Solopova, A. Abakumov, S. Turner, M. Hanfland, E. Bykova, M. Bykov, C. Prescher, V. B. Prakapenka, S. Petitgirard, I. Chuvashova, B. Gasharova, Y. L. Mathis, P. Ershov, I. Snigireva, and A. Snigirev, Terapascal static pressure generation with ultrahigh yield strength nanodiamond, Sci Adv. **2**, e1600341 (2016).

[23] A. Dewaele, P. Loubeyre, F. Occelli, O. Marie, and M. Mezouar, Toroidal diamond anvil cell for detailed measurements under extreme static pressures, Nat. Commun. **9**, 2913 (2018).

[24] T. Sakai, T. Yagi, T. Irifune, H. Kadobayashi, N. Hirao, T. Kunimoto, H. Ohfuji, Kawaguchi-Imada S, Y. Ohishi, S. Tateno, and K. Hirose, High pressure generation using double-stage diamond anvil technique: Problems and equations of state of rhenium, High Pressure Res. **38**, 107 (2018).

[25] K. Umemoto, R. M. Wentzcovitch, and P. B. Allen, Dissociation of $MgSiO_3$ in the cores of gas giants and terrestrial exoplanets, Science **311**, 983 (2006).

[26] K. Umemoto and R. M. Wentzcovitch, Two-stage dissociation in $MgSiO_3$ post-perovskite, Earth Planet. Sci. Lett. **311**, 225 (2011).

[27] K. Umemoto, R. M. Wentzcovitch, S. Wu, M. Ji, C. Z. Wang, and K. M. Ho, Phase transitions in $MgSiO_3$ post-perovskite in super-Earth mantles, Earth Planet. Sci. Lett. **478**, 40 (2017).

[28] H. Niu, A. R. Oganov, X. Q. Chen, and D. Li, Prediction of novel stable compounds in the Mg-Si-O system under exoplanet pressures, Sci. Rep. **5**, 18347 (2015).

[29] K. Hakim, A. Rivoldini, T. Van Hoolst, S. Cottenier, J. Jaeken, T. Chust, and G. Steinle-Neumann, A new *ab initio* equation

of state of hcp-Fe and its implication on the interior structure and mass-radius relations of rocky super-Earths, Icarus **313**, 61 (2018).

[30] A. P. van den Berg, D. A. Yuen, K. Umemoto, M. H. G. Jacobs, and R. M. Wentzcovitch, Mass-dependent dynamics of terrestrial exoplanets using ab initio mineral properties, Icarus **317**, 412 (2019).

[31] K. Hirose, K. Kawamura, Y. Ohishi, S. Tateno, and N. Sata, Stability and equation of state of $MgGeO_3$ post-perovskite phase, Am. Mineral. **90**, 262 (2005).

[32] H.-Z. Liu, J. Chen, J. Hu, C. D. Martin, D. J. Weidner, D. Häusermann, and H.-K. Mao, Octahedral tilting evolution and phase transition in orthorhombic $NaMgF_3$ perovskite under pressure, Geophys. Res. Lett. **32**, L04304 (2005).

[33] E. Ito, D. Yamazaki, T. Yoshino, H. Fukui, S. Zhai, A. Shatzkiy, T. Katsura, Y. Tange, and K. Funakoshi, Pressure generation and investigation of the post-perovskite transformation in $MgGeO_3$ by squeezing the Kawai-cell equipped with sintered diamond anvils, Earth Planet. Sci. Lett. **293**, 84 (2010).

[34] T. Yagi, T. Suzuki, and S. Akimoto, New high-pressure polymorphs ion sodium halides, J. Phys. Chem. Solids **44**, 135 (1983).

[35] J. Haines, J. M. Leger, F. Gorelli, D. D. Klug, J. S. Tse, and Z. Q. Li, X-ray diffraction and theoretical studies of the high-pressure structures and phase transitions in magnesium fluoride, Phys. Rev. B **64**, 134110 (2001).

[36] J. P. Perdew and A. Zunger, Self-interaction correction to density-functional approximations for many-electron systems, Phys. Rev. B **23**, 5048 (1981).

[37] D. Vanderbilt, Soft self-consistent pseudopotentials in a generalized eigenvalue formalism, Phys. Rev. B **41**, 7892(R) (1990).

[38] R. M. Wentzcovitch, Invariant molecular-dynamics approach to structural phase transitions, Phys. Rev. B **44**, 2358 (1991).

[39] R. M. Wentzcovitch, J. L. Martins, and G. D. Price, *Ab Initio* Molecular Dynamics with Variable Cell Shape: Application to $MgSiO_3$, Phys. Rev. Lett. **70**, 3947 (1993).

[40] S. Baroni, S. de Gironcoli, A. Dal Corso, and P. Giannozzi, Phonons and related crystal properties from density-functional perturbation theory, Rev. Mod. Phys. **73**, 515 (2001).

[41] P. Giannozzi, S. de Gironcoli, P. Pavone, and S. Baroni, *Ab initio* calculation of phonon dispersions in semiconductors, Phys. Rev. B **43**, 7231 (1991).

[42] D. Wallace, *Thermodynamics of Crystals* (Wiley, Hoboken, NJ, 1972).

[43] T. Qin, Q. Zhang, R. M. Wentzcovitch, and K. Umemoto, qha: A Python package for quasiharmonic free energy calculation for multi-configuration systems, Comput. Phys. Commun. **237**, 199 (2019).

[44] P. Giannozzi *et al.*, Quantum ESPRESSO: A modular and open-source software project for quantum simulations of materials, J. Phys.: Condens. Matter **21**, 395502 (2009).

[45] K. Umemoto and R. M. Wentzcovitch, Potential ultrahigh pressure polymorphs of ABX_3-type compounds, Phys. Rev. B **74**, 224105 (2006).

[46] F. Marumo and Y. Syono, The crystal structure of Zn_2SiO_4-II, a high-pressure phase of Willemite, Acta Cryst. B **27**, 1868 (1971).

[47] K. Umemoto, and R. M. Wentzcovitch, Multi-Mbar phase transitions in minerals, Rev. Mineral. Geochem. **71**, 299 (2010).

[48] See Supplemental Material at http://link.aps.org/supplemental/10.1103/PhysRevMaterials.3.123601 for the figures of vibrational and electronic densities of states.

[49] F. Coppari, R. F. Smith, J. H. Eggert, J. Wang, J. R. Rygg, A. Lazicki, J. A. Hawreliak, G. W. Collins, and T. S. Duffy, Experimental evidence for a phase transition in magnesium oxide at exoplanet pressures, Nat. Geosci. **6**, 926 (2013).

[50] M. J. Mehl, R. E. Cohen, and H. Krakauer, Linearized augmented plane wave electronic structure calculations for MgO and CaO, J. Geophys. Res. **93**, 8009 (1988).

[51] B. B. Karki, L. Stixrude, S. J. Clark, M. C. Warren, G. J. Ackland, and J. Crain, Structure and elasticity of MgO at high pressure, Am. Mineral. **82**, 51 (1997).

[52] A. R. Oganov, M. J. Gillan, and G. D. Price, *Ab initio* lattice dynamics and structural stability of MgO, J. Chem. Phys. **118**, 10174 (2003).

[53] Z. Wu, R. M. Wentzcovitch, K. Umemoto, B. Li, K. Hirose, and J.-C. Zheng, Pressure-volume-temperature relations in MgO: An ultrahigh pressure-temperature scale for planetary sciences applications, J. Geophys. Res. **113**, B06204 (2008).

[54] H. Dekura, T. Tsuchiya, and J. Tsuchiya, First-principles prediction of post-pyrite phase transitions in germanium dioxide, Phys. Rev. B **83**, 134114 (2011).

[55] T. Tsuchiya and J. Tsuchiya, Prediction of a hexagonal SiO_2 phase affecting stabilities of $MgSiO_3$ and $CaSiO_3$ at multi-megabar pressures, Proc. Natl. Acad. Sci. USA **108**, 1252 (2011).

[56] S. Wu, K. Umemoto, M. Ji, C. Z. Wang, K. M. Ho, and R. M. Wentzcovitch, Identification of post-pyrite phase transitions in SiO_2 by a genetic algorithm, Phys. Rev. B **83**, 184102 (2011).

[57] A. Kubo, B. Kiefer, G. Shen, V. B. Prakapenka, R. J. Cava, and T. S. Duffy, Stability and equation of state of the post-perovskite phase in $MgGeO_3$ to 2 Mbar, Geophys. Res. Lett. **33**, L12S12 (2006).

[58] K. Umemoto, R. M. Wentzcovitch, D. J. Weidner, and J. B. Parise, $NaMgF_3$: A low-pressure analog of $MgSiO_3$, Geophys. Res. Lett. **33**, L15304 (2006).

[59] K. Umemoto and R. M. Wentzcovitch, Prediction of an U_2S_3-type polymorph of Al_2O_3 at 3.7 Mbar, Proc. Natl. Acad. Sci. USA **105**, 6526 (2008).

[60] C. Jakymiw, L. Vocadlo, D. P. Dobson, E. Bailey, A. R. Thomson, J. P. Brodholt, I. G. Wood, and A. Lindsay-Scot, The phase diagrams of $KCaF_3$ and $NaMgF_3$ by ab initio simulations, Phys. Chem. Miner. **45**, 311 (2017).

[61] C. Xu, B. Xu, Y. Yang, H. Dong, A. R. Oganov, S. Wang, W. Duan, B. Gu, and L. Bellaiche, Prediction of a stable post-post-perovskite structure from first principles, Phys. Rev. B **91**, 020101(R) (2015).

[62] C. D. Martin, W. A. Crichton, H. Liu, V. Prakapenka, J. Chen, and J. B. Parise, Phase transitions and compressibility of $NaMgF_3$ (Neighborite) in perovskite- and post-perovskite-related structures, Geophys. Res. Lett. **33**, L11305 (2006).

[63] B. Grocholski, S.-H. Shim, and V. B. Prakapenka, Stability of the $MgSiO_3$ analog $NaMgF_3$ and its implication for mantle structure in superEarths, Geophys. Res. Lett. **37**, L14204 (2010).

[64] R. Dutta, E. Greenberg, V. B. Prakapenka, and T. S. Duffy, Phase transitions beyond post-perovskite in $NaMgF_3$ to 160 GPa, Proc. Natl. Acad. Sci. USA **116**, 19324 (2019).

[65] R. M. Wentzcovitch, Y. G. Yu, and Z. Wu, Thermodynamic properties and phase relations in mantle minerals investigated by first principles quasiharmonic theory, Rev. Mineral. Geochem. **71**, 59 (2010).

[66] Y. Zhao, D. J. Weidner, J. Ko, K. Leinenweber, X. Liu, B. Li, Y. Meng, R. E. G. Pacalo, M. T. Vaughan, Y. Wang, and A. Yeganeh-Haeri, Perovskite at high P-T conditions: An in situ synchrotron X ray diffraction study of $NaMgF_3$ perovskite, J. Geophys. Res. **99**, 2871 (1994).

[67] K. Umemoto and R. M. Wentzcovitch, Two-stages dissociation of $NaMgF_3$ post-perovskite: A potential low-pressure analog of $MgSiO_3$ at multi-Mbar pressures, JPS Conf. Proc. **4**, 011002 (2015).